IEEE Access
Multidisciplinary | Rapid Review | Open Access Journal

Received June 6, 2019, accepted June 10, 2019, date of publication June 13, 2019, date of current version July 1, 2019.

Digital Object Identifier 10.1109/ACCESS.2019.2922784

Research on Thermal Characteristics of Internal Ventilated Paths in Compact Medium High-Voltage Motor Based Fluid Network Decoupling

MENGMENG AI, YANG YANG, YONGMING XU, ZHENBO LI, LISHEN XU, AND WENCHENG WANG

College of Electrical and Electronic Engineering, Harbin University of Science and Technology, Harbin 150080, China

Corresponding author: Yongming Xu (xuyongming@hrbust.edu.cn)

This work was supported by the National Natural Science Foundation of China under Grant 51207036.

ABSTRACT Aiming at the problem that it is difficult to model and analyze the thermal effect of large motors as a whole, a method based on fluid network decoupling is proposed to solve the global thermal effect of large motors. Taking YJKK500-4 2500-kW compact medium-sized high-voltage motor as an example, combined with the internal structure and the actual size of the motor, and using the flow-heat coordination mechanism and the fluid network, the whole internal ventilated paths of motor are divided into four equal pressure regions: end, stator-rotor, end, and internal fan according to the magnitude of pressure. The reasonable basic assumptions and boundary conditions are selected to link each region, which can avoid the problem that the inlet boundary condition is difficult to give. After that, the internally ventilated paths are modeled and analyzed, and the fluid flow and temperature in each region of the internally ventilated paths are obtained. Combined with the experimental data, the calculation results are all within the error. The rationality and correctness of the method used in the paper are confirmed, which solves the problem that the ordinary computer cannot calculate the huge model of large motor and provides a basis for the calculation of similar motor in the future.

INDEX TERMS YJKK compact medium high-voltage motor (YJKK), fluid network decoupling, internal ventilated paths, fluid characteristics, thermal effect.

I. INTRODUCTION

When the motor realizes the electromechanical energy conversion in the actual operation, it will produce loss in its interior at the same time. Loss not only affects the overall efficiency of the motor, but also increases the temperature rise of the motor, affects the service life of the motor insulation material and limits the output of the motor [1], [2]. Therefore, in order to improve the ventilation and heat transfer capacity of the motor, in recent years, many motor designers made fruitful research work on the fluid flow and thermal effect inside the motor.

Nakahama T et al. studied the axial flow fan with lean blades, and explored the cooling performance of the combination of the ventilation resistance structure and the axial flow fan with lean blade [3]. Fu Yao et al. analyzed the three-dimensional fluid field in the rotating channel of the motor rotor cooling system by numerical simulation method. Based on the analysis of the results, the structure of the channel was improved to reduce the flow loss [4]. Xing Junqiang et al. studied the air friction loss of high-speed permanent magnet motor rotor based on fluid flow theory, and discussed the influence of rotor speed, axial wind speed, air gap structure and surface roughness of rotor on wind friction loss, which provided a basis for reducing wind friction loss [5]. Ponomarev P et al. established lumped parameter thermal network, thermal static finite element model and computational fluid dynamics model of permanent magnet synchronous motor to study the potential and effectiveness of direct oil cooling, and concluded that computational fluid dynamics method can most accurately calculate the cooling effect [6]. Zhang Zhenhai et al. made a numerical analysis

The associate editor coordinating the review of this manuscript and approving it for publication was Xiaodong Sun.

of fluid distribution in cage induction wind turbines by using fluid flow knowledge, and discussed the influence of the axial ventilation ducts number of rotor on the uniform distribution of flow and velocity in the motor [7]. Yoo Wookyung et al. studied the fluid flow and heat transfer in the ventilation system of the generator rotor, and analyzed the influence of three different states on the heat transfer of the rotor [8]. Li Guangyu et al. optimized the centrifugal fan of high-voltage motor, and gave the optimization result of the external fan and its characteristic curve [9]. Wang Hongyu et al. analyzed the stator temperature distribution of hydroelectric generator based on the thermal-fluid coupling network model. The model compensated for the inaccuracy of some boundary conditions when calculating the stator region, and the temperature distribution of each part of the stator was given in detail [10]. Li Bin et al. established a physical model of three-dimensional thermal network of permanent magnet synchronous motor (PMSM) with an axial cooling system based on the law of the non-uniform distribution of fluid temperature in the axial cooling system, solved the asymmetric distribution of temperature in the axial direction of the motor, and compared with the results of finite element analysis, confirmed the accuracy of the three-dimensional thermal network analysis [11]. Moon S H et al. based on the theory of computational fluid dynamics, calculated the fluid distribution and temperature distribution of TEFC motor by finite element method, and put forward the optimization design of fluid distribution to reduce the highest temperature of the motor [12].

In summary, the research of temperature field and fluid field in large and medium-sized motors have been made a positive exploratory attempt to analyze by scholars, some valuable experience from practice and theory have been accumulated. However, there are still many imperfections which deserve further study, especially for the research of fluid and temperature fields of large motors mainly focuses on the local of the structure currently. If the whole area of the motor is studied, it will involve a large amount of calculation, which is difficult to achieve. But when the local of the structure is taken as the research object, the boundary conditions of the inlet are generally difficult to be given accurately, or to be assumed, or to be solved by an algorithm, which has certain influence on the analysis conclusion and has limitations [13], [14].

A method based on field-circuit combination is presented in the paper, the whole internal ventilated paths of YJKK500-4 2500 kW compact medium-sized high-voltage motor are divided into four equal pressure regions: end, stator-rotor, end and internal fan according to the magnitude of pressure. The reasonable basic assumptions and boundary conditions are selected to link each region, after that, each region of the internal ventilated paths is modeled and analyzed by the Flow-Heat synergistic mechanism, and the fluid flow and thermal effect in each region of the internal ventilated paths are analyzed. Combined with the experimental data, the calculation results are all within the error, which can confirm the rationality and correctness of the method that used in the paper. It can avoid the problem that the inlet boundary condition is difficult to give, which solves the problem that the ordinary computer cannot calculate the huge model of large motor, and provides a basis for the calculation of similar motor in the future.

II. METHODOLOGY

A. BASIC STRUCTURE OF YJKK MOTOR

Because of high power density, YJKK series motors have special structure, which adopt a closed self-fan shaft radial ventilation and heat dissipation structure. The ventilation system of YJKK motors is shown in Fig.1.

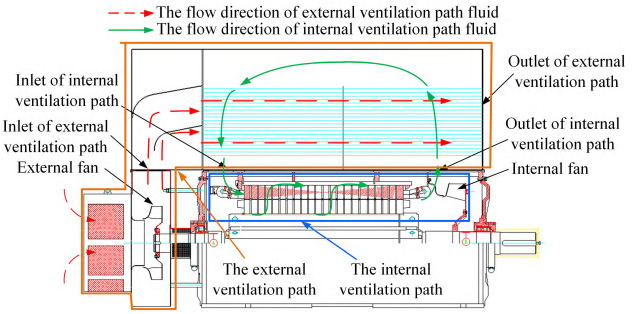

FIGURE 1. Ventilation system of YJKK series motor.

It can be seen from Fig. 1, the fluid in the internal ventilated path enters the motor through the inlet of the internal ventilated path on one side of the motor, and flows into the fluid area of the rotor and the bracket through the end of the stator and the balance rings of the rotor. Then, due to the rotation of the rotor bracket and the rotor, the fluid in the internal ventilated path is divided into two paths and flows along the bracket of the rotor and the radial ventilation channel.

In this paper, YJKK500-4, 2500kW compact medium-sized high-voltage asynchronous motors are used as research motors. The parameters of the main dimensions related to the ventilation system and its modeling are listed in Tab. 1.

B. MATHEMATICAL MODELS

The analysis of fluid flow and heat transfer characteristics in YJKK Motors should follow the laws of conservation of mass, momentum and energy [15]–[17]. It is considered that the fluid inside and outside the YJKK motor is incompressible viscous fluid in the calculation process [18]. The laws of physical conservation and the corresponding governing equations of fluid in YJKK motor are given.

The continuity mass equation of incompressible fluid unsteady flow in YJKK motor can be expressed as

$$\frac{\partial v_x}{\partial x} + \frac{\partial v_y}{\partial y} + \frac{\partial v_z}{\partial z} = 0 \tag{1}$$

where v_x, v_y, v_z are the components of velocity vector in the direction of x, y, z.

The vector form of Navier-Stokes momentum equation for incompressible viscous fluid in YJKK motor can be

TABLE 1. Basic parameters of the prototype.

Parameter	Value	Parameter	Value
Rated power(kW)	2500	Rated voltage(kV)	6
Rated speed(r/min)	1480	Slip ratio	0.013
Pole	4	Stator outer diameter(mm)	900
Stator inner diameter(mm)	560	Rotor inner diameter(mm)	310
Rotor outer diameter(mm)	553.6	Number of stator slot(mm)	60
Number of rotor slots	72	Core length(mm)	900
Ventilation Number	14	Efficiency	0.966
Power factor	0.84	Insulation grade	F（155℃）
Stator winding connection	Y	Air gap thickness(mm)	1.8
Inlet area of inner wind path(mm^2)	920*400	Outlet area of inner wind path(mm^2)	920*299
Number of cooling pipes	750	Specification of cooling pipes (Length*Diameter(mm^2))	1800*20
Specification of stator ventilation ditch (length* width *height(mm^3))*Number		(4*8*160)*60	
Specification of rotor ventilation ditch(length*width*height(mm^3))*Number		(4*8*65)*54 +(4*8*160)*18	

expressed as

$$\frac{\partial(\rho u)}{\partial t} = -\nabla p + u\Delta v + pF \tag{2}$$

where ρ is density; t is time; p is pressure on the microelement; F is physical force on the microelement; μ is dynamic viscous coefficient; v is the fluid velocity.

The corresponding energy conservation equation in YJKK motor is

$$\frac{\partial(\rho T)}{\partial t} + div(\rho u T) = div(\frac{\lambda}{c} grad\, T) + S_T \tag{3}$$

where T is temperature; λ is thermal conductivity; c is specific heat capacity; S_T is viscous dissipation term.

If the fluid in YJKK motor is in turbulent state, an additional turbulent transport equation is needed to describe it. According to the theory of fluid mechanics, the standard $k-\varepsilon$ equation model is used to describe the fluid. When the fluid is incompressible and stable, the general governing equation is adopted [19].

$$\begin{cases} \dfrac{\partial(\rho k)}{\partial t} + \dfrac{\partial(\rho k u_i)}{\partial x_i} = \dfrac{\partial}{\partial x_j}[(\mu + \dfrac{\mu_t}{\sigma_k})\dfrac{\partial k}{\partial x_j}] \\ \qquad +G_k + G_b - \rho\varepsilon - Y_M + S_k \\ \dfrac{\partial(\rho\varepsilon)}{\partial t} + \dfrac{\partial(\rho\varepsilon u_i)}{\partial x_i} = \dfrac{\partial}{\partial x_j}[(\mu + \dfrac{\mu_t}{\sigma_\varepsilon})\dfrac{\partial \varepsilon}{\partial x_j}] \\ \qquad +C_{1\varepsilon} + \dfrac{\varepsilon}{k}(G_k + C_{3\varepsilon}G_b) - C_{2\varepsilon}\rho\dfrac{\varepsilon^2}{\lambda} + S_\varepsilon \end{cases} \tag{4}$$

where G_k is the turbulent kinetic energy generation term caused by the average velocity change rate; G_b is the generation term of turbulent kinetic energy caused by the pressure difference between the upper and lower surfaces of the fluid; Y_M is the variable of wave propagation in compressed turbulence; $C_{1\varepsilon}$, $C_{2\varepsilon}$, $C_{3\varepsilon}$, σ_k and σ_ε is the empirical constant, and according to the experiment and theory, it is recommended that the $C_{1\varepsilon} = 1.44$, $C_{2\varepsilon} = 1.92$, $C_\mu = 0.09$, $\sigma_k = 1.0$, $\sigma_\varepsilon = 1.3$; S_k and S_ε are user-defined sources.

C. BASIC ASSUMPTIONS

(1) The Reynolds number in the axial and radial ventilation and heat dissipation system of the motor is large, and the rotor and the bracket are rotated, so RNG $k-\varepsilon$ turbulence model is selected [20], [21];
(2) Ignoring the influence of buoyancy and gravity of fluid in the motor [22];
(3) The velocity of fluid movement in the motor is much less than that of sound, and its Mach number is relatively small, so it is treated as incompressible fluid [23];
(4) The axial velocity of the fluid in the air gap has little effect on the fluid flow in the motor, so the axial initial velocity is ignored;
(5) The fluid flow and distribution in steady state are analyzed and solved, so the fluid flow is treated as steady flow [24].
(6) The thermal conductivity of the interlayer insulation of winding and the main insulation of winding are treated as the same [25].

D. BOUNDARY CONDITIONS

(1) The inlet of the internal wind path is set to velocity inlet boundary condition, the inlet velocity is 6.5m/s, the inlet temperature is 50°, the outlet of the internal wind path is set to pressure outlet boundary condition, and the outlet static pressure is set to 0;
(2) Rotor and bracket are rotating parts, so their boundary conditions are set to rotating wall;
(3) MRF is used to simulate the rotating parts;
(4) The fluid-solid interface is regarded as the coupling interface.

E. FUILD FIELD DECOUPLING ANALYSIS

The internal ventilated path of the motor mainly includes end, stator and rotor, end and internal fan, etc. and the physical model is shown in Fig.2.

Because the structure of YJKK motor is complex and the size of the motor is large, it is almost impossible to model and analyze the motor as a whole. Combined with past experts and scholars' research papers, the whole internal ventilated paths of motor can be divided into 4 equal pressure regions, and the reasonable basic assumptions and boundary conditions are selected to link each region. The fluid network of its internal ventilated path is shown in Fig.3.

The steps of fluid network decoupling in Fig.3 are that: according to the actual size of the motor and the basic assumptions, a three-dimensional physical model of the motor end region is established to solve the fluid flow and thermal effects. Then, the physical model of the stator and

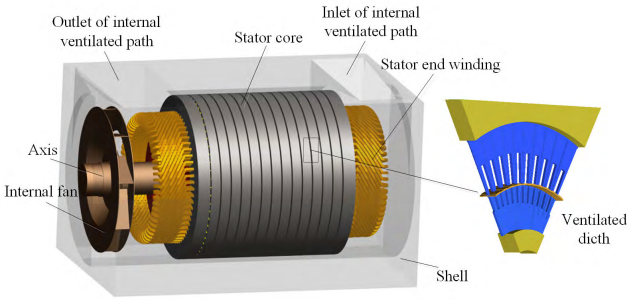

FIGURE 2. The 3D model of internal ventilated path.

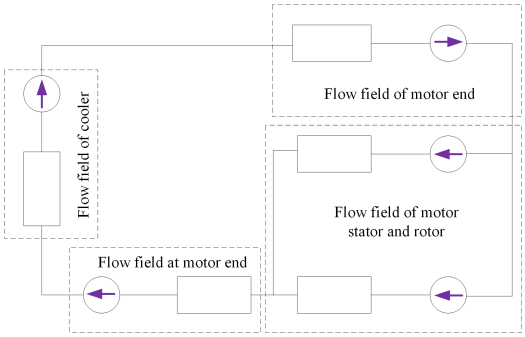

FIGURE 3. The fluid network of internal ventilated path.

rotor of the motor is established, and the results of the end of the motor are used as the initial boundary conditions to calculate the fluid flow in the whole stator and rotor region. Based on the fluid distribution, the fluid-solid coupling calculation model of the stator and rotor region is established, and the temperature distribution in the stator and rotor region is analyzed. Finally, the calculation model of the end and the cooler are established. The results of the stator and rotor region are used as the initial boundary conditions of the end and the cooler to carry out detailed numerical analysis and calculation. In the whole calculation process, the field-circuit combination method is adopted, and the Flow-Heat coordination mechanism is used to improve the accuracy and accuracy of the calculation results. Detailed solutions will be provided in section III.

F. AUXILIARY FINITE ELEMENT SOFTWARE SETTING

Based on the above description, the whole internal ventilated paths of motor are divided into four equal pressure regions: end, stator-rotor, end and internal fan according to the magnitude of pressure. the heat transfer characteristics is analyzed by using the finite element Ansys software. Following is a description of the finite element software grid, solver and algorithm [26]–[28]:

1. In finite element calculation, the grid quality directly determines whether the success of the calculation is, especially in special or fine structures, which need to be handled separately. In the paper, octree method is used to divide tetrahedral meshes of the model.
2. Solver is the core of finite element simulation. Coupled solver is chosen in this paper to solve all control equations simultaneously and solve all variables jointly.
3. The algorithm of the solver is the strategy adopted in solving. In order to accelerate the convergence process, SIMPLEC algorithm is chosen in this paper.

III. FLUID FLOW AND TEMPERATURE ANALYSIS OF INTERNAL VENTILATED PATHS IN MOTOR

A. RESEARCH ON FLUID FLOW AND THERMAL EFFECT IN END REGION

Based on the flow-heat coordination mechanism, a fluid-solid coupling calculation model in the end region is established as shown in Fig.4.

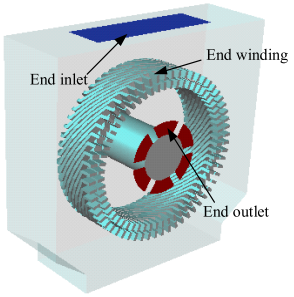

FIGURE 4. The fluid-solid coupling calculation model of end region.

The fluid flow and temperature distribution were calculated and analyzed in the paper, and the fluid flow in the end was obtained. The figure of fluid velocity vectors and temperature are shown in Figs.5 and 6.

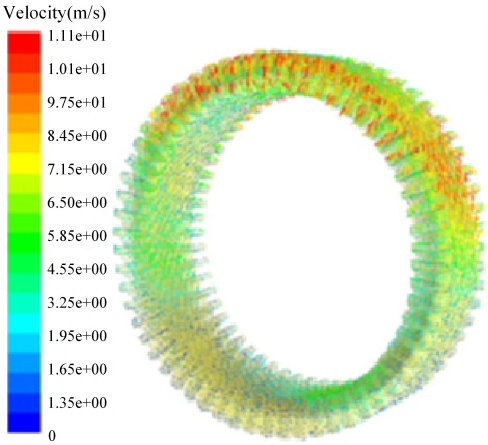

FIGURE 5. The fluid velocity vector of end region.

It can be seen from Fig.5, the velocity distribution on the stator end winding surface is not uneven. The speed of winding surface near the end inlet is higher than that of other places, up to 11.1m/s. This is due to the fact that the end winding near the end inlet is influenced by the velocity of the air inlet, correspondingly, the temperature distribution of the

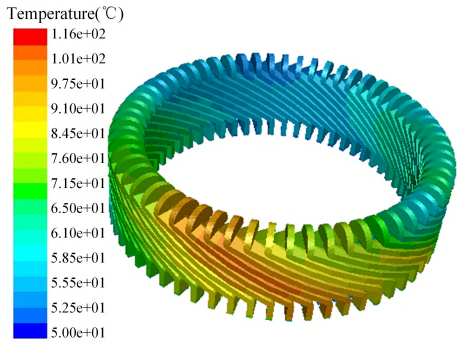

FIGURE 6. Temperature distribution of end region.

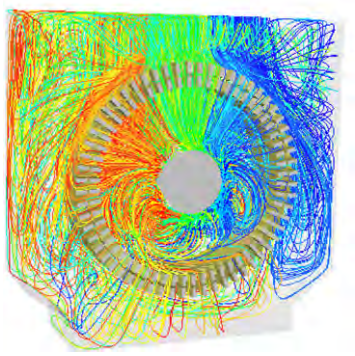

FIGURE 7. The fluid trajectories of end region.

end winding is uneven from Fig. 6, and the temperature of the end winding near the end entrance is lower, which is 53°; the temperature of the end winding away from the end inlet is higher, which is 113°. It also shows that the cooling effect is better when the speed of wind is high.

Then the fluid trajectory is explored as shown in Fig.7.

It can be seen from Fig.7, the vortex will occur in the place of sudden deformation location during the flow of fluid. The generation of vortex will increase the loss and noise pollution of the motor, which can affect the efficiency and performance of the motor. Therefore, it is necessary to minimize the use of sudden deformation of the structure in the process of motor design, the vortex phenomenon should be effectively reduced and the overall performance of the motor can be improved.

B. RESEARCH ON FLUID-SOILD COUPLING IN STATOR AND ROTOR REGION OF MOTOR

Because of the complex structure of stator and rotor region, it is difficult to directly analyze the coupling of fluid field and temperature field. Therefore, based on the Flow-Heat coordination mechanism, the fluid field calculation model of the stator-rotor region is established, and the fluid flow and flow distribution in the whole stator-rotor region are obtained by calculation and analysis, which can provide a solid theoretical foundation for the next calculation of temperature distribution in combination and its fluid distribution. The structure of stator and rotor fluid field is shown in Fig.8.

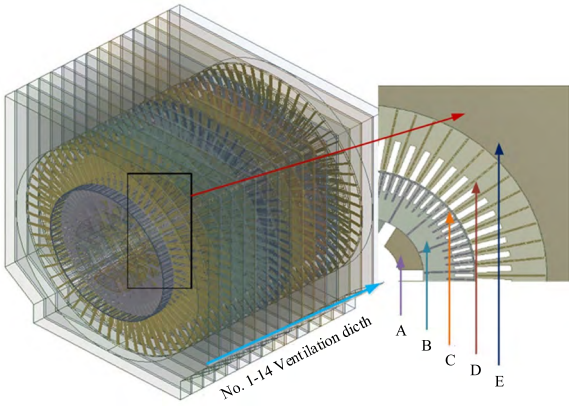

FIGURE 8. Structure of stator and rotor fluid domain. A. Bracket fluid region; B. Rotor ventilation duct fluid region; C. Air gap fluid region; D. Stator ventilation ditch fluid region; E. Shell fluid region.

It can be seen from Fig.8, the No.1 ventilation ditch is near the inlet of the bracket, and then named until No.14 ventilation ditch in turn.

When studying the fluid flow in the stator and rotor regions, multi-reference coordinates are used to analyze the rotating parts such as the bracket fluid region and the rotor ventilation ditch fluid region, and RNG turbulence model is selected as the solution model. The flow distribution in the No.1 ventilation ditch to No.14 ventilation ditch of the internal wind path is obtained through calculation and solution, as shown in Fig.9.

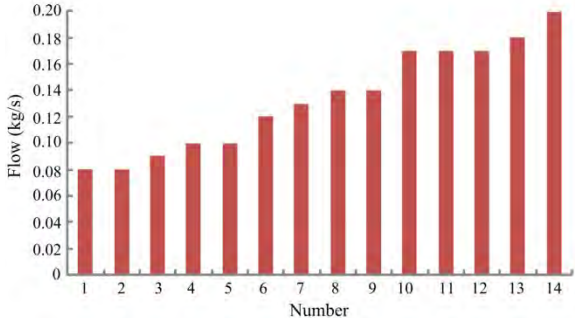

FIGURE 9. The flow distribution of ventilation duct in internal ventilated path.

It can be found from Fig.9 that the flow rate in each ventilation ditch of the internal wind path increases with the increase of the number of ventilation ditches. This is because the paths of the fluids flow in the ventilation ditches are different in the rotating bracket. With the decrease of the number of ventilation ditches, the fluids flow paths through the rotating bracket is longer.

Considering that the ventilation and cooling structures in the stator and rotor regions are identical, therefore, a ventilation ditch and half of its two adjacent cores are modeled in this section, which can greatly reduce the amount of calculation and improve the efficiency of research. The fluid-solid

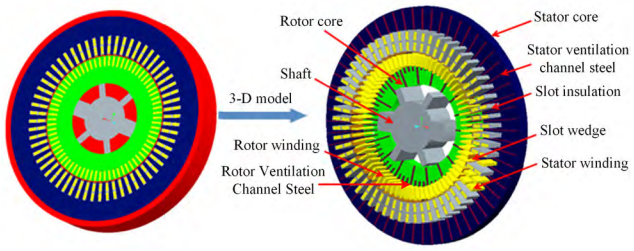

FIGURE 10. Fluid-solid coupling calculation model of stator and rotor.

coupling calculation model of stator and rotor is shown in Fig.10.

The intrinsic factor of motor heating is that it produces various losses in operation, and these losses ultimately exist in the form of heat energy. In this paper, all kinds of losses of motor in operation are obtained by on-site measurement. which are shown in Tab. 2.

TABLE 2. Test data of the motor loss distribution.

Loss	Value/W	Loss	Value/W
Stator copper loss	15978	No-load loss	39470
Stator iron loss	27819	Rotor aluminum consumption loss	21916
Stray Loss	12940	Mechanical loss	10688

Based on the field-circuit combination method and the fluid-thermal synergistic mechanism, the fluid-solid coupling calculation model of each section ventilation ditch and two sides of the stator core is calculated to find the highest temperature in the stator and rotor core region in turn. Through the analysis of the temperature distribution in each core section, it can be found that the highest temperature rise in the stator and rotor region occurs in the seventh ventilation ditch and the iron core on both sides. The velocity and temperature of the fluid in the seventh ventilation ditch are shown in Fig 11.

It can be seen from Fig.11 (1), the speed of the rotor ventilation ditch side is larger than that of the stator ventilation ditch side. This is because when the rotor ventilation channel steel rotates, it is equivalent to the fan, which accelerates the flow of fluid in the rotor ventilation channel side. The local magnification at A in Fig.11 shows that the distribution of fluid in the stator ventilation ditch is uneven, this is due to the rotation of the rotor ventilation channel steel, which results in the velocity distribution uneven of the fluid in the stator ventilation channel. It can be seen that the eddy current occurs from Fig.11 B when the fluid flows through the back of the stator copper bar in the stator ventilation ditch. The eddy current phenomenon seriously affects the cooling effect of motor, and also produces certain noise pollution, which affects the overall performance of the motor. Fig.11 (2) shows that the highest temperature occurs at the stator winding, up to 115°, and the temperature distribution on the stator

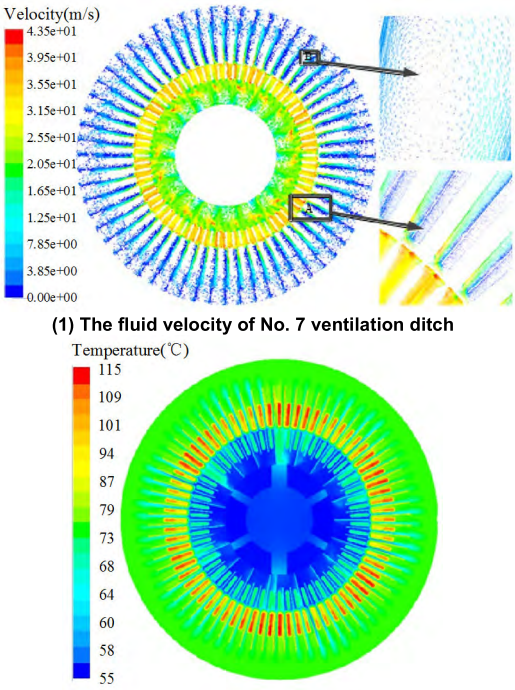

(1) The fluid velocity of No. 7 ventilation ditch

(2) Temperature distribution of No.7 ventilation ditch

FIGURE 11. The fluid velocity and temperature distribution of No. 7 ventilation ditch. (1) The fluid velocity of No. 7 ventilation ditch. (2) Temperature distribution of No.7 ventilation ditch.

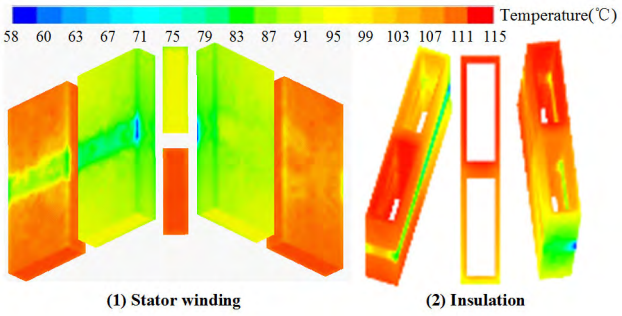

FIGURE 12. Temperature distribution in the stator of No. 7 iron core. (1) Stator winding. (2) Insulation.

winding is not uneven; the temperature changes in the stator ventilation ditch fluid area and the bracket fluid area are not large. Therefore, stator winding, slot wedge and insulation need be analyzed in detail, as shown in Fig.12.

It can be seen From Fig.12 (1) that the upper winding temperature of the stator is low, basically around 96°, while the lower winding temperature is high, about 110°. The reason is that the fluid speed which just enters the stator ventilation ditch through the air gap from the rotor ventilation ditch is higher and the cooling effect is better. Both upper and lower winding have lower temperature in their middle position, which is due to the fact that the stator winding in the middle position are located in the stator ventilation ditch, and the flow velocity of the fluid is larger than that in other parts, and the cooling effect is better. The insulation

temperature distribution in Fig.12 (2) is also affected by this. The temperature distribution of insulation near the upper winding is low, while that near the lower winding is high. The insulation temperature at the middle ventilation ditch is the lowest, whose average temperature is 85°. This is due to the excess heat is taken away by the fluid flow in the ventilation ditch, which makes the insulation temperature at the middle ventilation ditch lower.

C. ANALYSIS OF END REGION NEAR THE OUTLET OF INTERNAL VENTILATED PATHS

According to the actual size of the motor, the model of the end region near the outlet of the internal ventilated paths is established. The calculation results of stator and rotor regions are taken as the initial boundary conditions, and the fluid flow and thermal effects in this region are calculated. The physical model of the inner fan is shown in Fig.13.

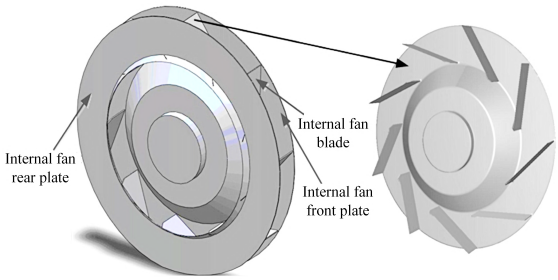

FIGURE 13. Three-dimensional physical model of internal fan.

Through numerical analysis and calculation, the fluid flow and thermal effect in the end region are obtained. The velocity vector of the internal fan is shown in Fig.14.

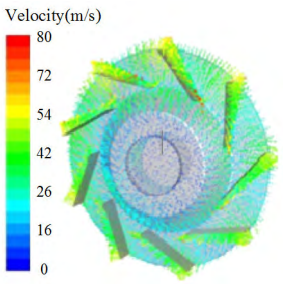

FIGURE 14. Velocity vector of internal fan.

IV. EXPERIMENTAL VERIFICATION

In order to verify the accuracy and rationality of this study, the temperature rise test of the motor is carried out. PT100 double platinum thermal resistance is selected as the measuring element, which is placed at the highest temperature point calculated in this paper, and the free end of three points is connected to the temperature measuring instrument through the temperature measuring line. The data of motor temperatures at different points are passed and recorded through the A/D

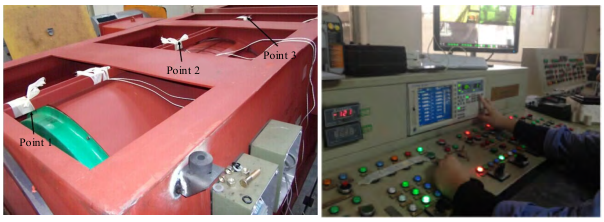

FIGURE 15. The experiment platform. (a) Test prototype. (b) Test installation.

datalogger with higher precision. The figure of temperature rise test is shown in Fig.15.

The final steady-state average value is taken as the test data in the experiment, and the comparison between the test data and the theoretical calculation value is shown in Tab 3.

TABLE 3. Comparison between theoretical calculated values and experimental measurements.

	Simulation value	Experimental value	Error
Maximum temperature of stator winding	115°C	120.1°C	4.4%

It can be found that the theoretical calculation value is low, which is due to simplifying some assumptions in modeling and calculation. But the error between them is within the allowable range of engineering practice and meets the actual needs. The results verify the accuracy of the model and the method selected in this paper.

V. CONCLUSIONS

Based on the method of fluid network decoupling, taking YJKK500-4, 2500kW motor as an example, the whole internal ventilated paths of the motor are decoupled into 4 equal pressure regions, and using the Flow-Heat synergistic mechanism, the internal ventilated paths are modeled and calculated, and the fluid flow and thermal effects in each region of the internal ventilated paths of the motor are solved. Combined with the experimental data, the calculation results are all within the error. However, there are still imperfections in the research, and we hope that we can continue to further explore and optimize the motor heat transfer characteristic.

REFERENCES

[1] D. Tan, H. Xue, K. Yang, A. Li, and H. Wang, "Study on the thermal characteristics of in-wheel motor drive system based on driving cycles," *IEEE Access*, vol. 7, pp. 14463–14471, 2019.
[2] X. Sun, B. Su, S. Wang, Z. Yang, G. Lei, J. Zhu, and Y. Guo, "Performance analysis of suspension force and torque in an IBPMSM with V-shaped PMs for flywheel batteries," *IEEE Trans. Magn.*, vol. 54, no. 11, Nov. 2018, Art. no. 8105504.
[3] T. Nakahama, D. Biswas, K. Kawano, and F. Ishibashi, "Improved cooling performance of large motors using fans," *IEEE Trans. Energy Convers*, vol. 21, no. 2, pp. 324–331, Jun. 2006.
[4] F. Yao, W. Tonggu, C. Gang, X. Wei, and H. Ming, "Flow analysis and structure improvement on the ventilation cooling system in the electric machine rotor," *J. Eng. Thermophys.*, vol. 29, no. 10, pp. 1679–1681, 2008.

[5] X. Junqiang, W. Fengxiang, Z. Dianhai, and K. Xiaoguang, "Research on rotor air friction loss of high-speed permanent magnet machines," *Chin. J. Electr. Eng.*, vol. 30, no. 27, pp. 14–19, 2010.
[6] P. Ponomarev, M. Polikarpova, and J. Pyrhönen, "Thermal modeling of directly-oil-cooled permanent magnet synchronous machine," in *Proc. 20th Int. Conf. Elect. Mach.*, Marseille, France, vol. 5, Sep. 2012, pp. 1882–1887.
[7] Z. Zhenhai, C. Changchun, C. Zhengbing, and S. Shiliang, "Ventilation structure optimization analysis of high-power density squirrel cage induction wind power generator," *Elect. Mach. Control. Appl.*, vol. 42, no. 4, pp. 53–57, 2015.
[8] W. Yoo, S. Jeon, C. Son, J. Yang, D. Ahn, S. Kim, K. Hwang, and S. Ha, "Full surface heat transfer characteristics of rotor ventilation duct of a turbine generator," *Appl. Thermal Eng.*, vol. 94, pp. 385–394, Feb. 2016.
[9] L. Guangyu, Y. Liqiang, Z. Zhengming, and W. Shuping, "Optimized design of high-efficiency AC motor external fan by computational fluid dynamic method," *Adv. Technol. Electr. Eng. Energy*, vol. 33, no. 11, pp. 24–28, 2014.
[10] W. Hongyu, L. Ming, L. Yingli, S. Pengsheng, and W. Xianghong, "Research on the nonlinear thermal-liquid coupled network model of whole stator of three-gorge generator," *Chin. J. Elect. Eng.*, vol. 28, no. 8, pp. 136–142, 2008.
[11] L. Bin, S. Jingcheng, and L. Hua, "Three dimensional thermal network model of permanent magnet synchronous machine equipped with axial ventilation system," *J. Tianjin Univ. (Natural Sci. Eng.)*, vol. 49, no. 11, pp. 1161–1166, 2016.
[12] S.-H. Moon, J.-H. Yun, W.-G. Kim, and J.-P. Kim, "Thermal-flow analysis and cooling performance enhancement of a totally enclosed fan-cooled motor," in *Proc. Int. Conf. Elect. Mach. Syst.*, Busan, South Korea, vol. 29, Oct. 2013, pp. 2028–2030.
[13] Y. Xu, Y. Jia, M. Ai, and Y. Wang, "Heat transfer characteristics of external ventilated path in compact high-voltage motor," *Int. J. Heat Mass Transf.*, vol. 124, pp. 1136–1146, Sep. 2018.
[14] Y. Xu, M. Ai, and D. Tao, "Investigation of the heat characteristic based on the exergy destruction rate for high power density motor," in *Proc. 20th Int. Conf. Elect. Mach. Syst.*, Sydney, NSW, Australia, Aug. 2017, pp. 1–5.
[15] P. Liang, Y. Pei, L. Gan, and F. Chai, "Research of temperature field modeling for high power-density in-wheel motor," *Trans. China Electrotech. Soc.*, vol. 30, no. 14, pp. 170–176, 2015.
[16] Z. Jianzhong and J. Yongjiang, "Thermal analysis of constant frequency double rotor permanent magnet generator based on equivalent thermal network method," *Trans. China Electrotech. Soc.*, vol. 30, no. 2, pp. 87–97, 2015.
[17] X. Yunyan, H. Yongsen, X. Yongming, and A. Mengmeng, "Analyzing temperature rise and fluid flow of high-power-density and high-voltage induction motor in the starting process," *IEEE Access*, vol. 7, pp. 35588–35595, 2019.
[18] W. Liguo, Z. Fengna, L. Xin, X. Zhuang, X. Dianguo, and D. Hui, "Temperature identification of electric submersible motor based on perturbation analysis of therodynamic parameters," *Trans. China Electrotech. Soc.*, vol. 26, no. 6, pp. 7–11, 2011.
[19] J. Wen and J. Zheng, "Numerical analysis of the external wind path for medium-size high-voltage asynchronous motors," *Appl. Therm. Eng.*, vol. 90, pp. 869–878, Nov. 2015.
[20] D. A. Staton and A. Cavagnino, "Convection heat transfer and flow calculations suitable for electric machines thermal models," *IEEE Trans. Ind. Electron.*, vol. 55, no. 10, pp. 3509–3516, Oct. 2008.
[21] H. Feiyang *et al.*, "Calculation and analysis on stator ventilation structure of different optimum proposal in air-cooled turbogenerator," *Chin. J. Electr. Eng.*, vol. 30, no. 6, pp. 69–74, 2010.
[22] X. Yongming, A. Mengmeng, and Z. Fang, "Oil circulation system inside submersible motor on heat transfer of submersible motor," *J. Elect. Mach. Control*, vol. 23, no. 1, pp. 80–88, 2019.
[23] L. Weili, Y. Xuefeng, and G. Debao, "Calculation and analysis of fluid flow and heat transfer of air-cooled turbo-generator with multipath ventilation," *Trans. China Electrotech. Soc.*, vol. 24, no. 12, pp. 24–31, 2009.
[24] D. Kaisong, Z. Yao, and L. Zhen, "Steady flow analysis of tubular turbine," *Large Electr. Mach. Hydraulic Turb.*, no. 1, pp. 39–43 and 47, Jan. 2015.
[25] L. Weili, C. Junci, and Z. Xiaochen, "Electrothermal analysis of induction motor with compound cage rotor used for PHEV," *IEEE Trans. Ind. Electron.*, vol. 57, no. 2, pp. 660–668, Feb. 2010.
[26] X. Sun, K. Diao, G. Lei, L. Chen, Y. Guo, and J. Zhu, "Study on segmented-rotor switched reluctance motors with different rotor pole numbers for BSG system of hybrid electric vehicles," *IEEE Trans. Veh. Technol.*, to be published. doi: 10.1109/TVT.2019.2913279.
[27] Y. Xiwei, M. Dawei, and L. Qiong, "Transient analysis of purging process of positive pressure explosion-proof motor based on multi-component fluid field," *J. Elect. Mach. Control*, vol. 23, no. 4, pp. 49–55, 2019.
[28] X. Liu and W. N. Fu, "A dynamic dual-response-surface methodology for optimal design of a permanent-magnet motor using finite-element method," *IEEE Trans. Magn.*, vol. 52, no. 3, Mar. 2016, Art. no. 7204304.

MENGMENG AI was born in Harbin, China, in 1991. He received the Ph.D. degree. He was a Lecturer with the College of Electrical and Electronic Engineering, Harbin University of Science and Technology, in 2017. He has presided over or participated in three national, provincial, and departmental scientific research projects and published 11 academic papers (more than nine papers were included by the SCI and EI). He holds ten patents. His research interests include the optimum design of motor, numerical calculation of integrated physical field in motor, and research on local overheating and fluid field of super large transformer.

YANG YANG was born in Heilongjiang, China, in 1982. She received the M.D. degree in electrical machine and electrical apparatus from the Harbin University of Science and Technology, in 2012, where she was an Assistant Research Fellow with the College of Electrical and Electronic Engineering. Her research interests include the design of special motor and numerical calculation of integrated physical field in motor.

YONGMING XU was born in Shuozhou, Shanxi, China, in 1979. He received the Ph.D. degree in electrical machine and electrical apparatus from the Harbin University of Science and Technology, in 2008, where he has been a Professor with the College of Electrical and Electronic Engineering, since 2013. His research interests include the design of special motor, numerical calculation of integrated physical field in motor, and research on local overheating and fluid field of super large transformer.

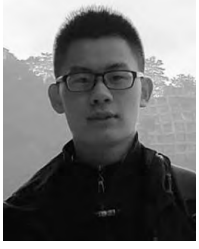

ZHENBO LI was born in Harbin, China, in 1999. He joined the Harbin University of Science and Technology, Harbin, China, in 2017, where he is currently pursuing the bachelor's degree in electrical engineering. He has participated in the provincial scientific research projects. He holds three patents. His research interest includes numerical calculation of integrated physical field in motor.

LISHEN XU was born in Suihua, China, in 2000. He joined the Harbin University of Science and Technology, Harbin, China, in 2018, where he is currently pursuing the bachelor's degree in electrical engineering. He has participated in a provincial scientific research projects. He holds three patents. His research interest is numerical calculation of integrated physical field in motor.

WENCHENG WANG was born in Shandong, China, in 1998. He joined the Harbin University of Science and Technology, Harbin, China, in 2016, where he is currently pursuing the bachelor's degree in electrical engineering. He has participated in a provincial scientific research projects. He holds three patents. His research interest includes numerical calculation of integrated physical field in motor.